

Article

Preparation and Properties of Various Magnetic Nanoparticles

Jana Drbohlavova ^{1,*}, Radim Hrdy ¹, Vojtech Adam ², Rene Kizek ², Oldrich Schneeweiss ³ and Jaromir Hubalek ¹

¹ Department of Microelectronics, Faculty of Electrical Engineering and Communication, Brno University of Technology, Údolní 53, 602 00 Brno, Czech Republic; E-Mails: hrdyr@email.cz (R.H.); hubalek@feec.vutbr.cz (J.H.)

² Department of Chemistry and Biochemistry, Faculty of Agronomy, Mendel University of Agriculture and Forestry, Zemědělská 1, 613 00 Brno, Czech Republic; E-Mails: ilabo@seznam.cz (V.A.); kizek@sci.muni.cz (R.K.)

³ Institute of Physics of Materials, Academy of Sciences of the Czech Republic, Žitkova 22, 616 62 Brno, Czech Republic; E-Mail: schneew@ipm.cz (O.S.)

* Author to whom correspondence should be addressed; E-Mail: drbohla@feec.vutbr.cz; Tel.: +420 541 146 163; Fax: +420 541 146 298

Received: 13 February 2009; in revised form: 23 March 2009 / Accepted: 30 March 2009 / Published: 30 March 2009

Abstract: The fabrications of iron oxides nanoparticles using co-precipitation and gadolinium nanoparticles using water in oil microemulsion method are reported in this paper. Results of detailed phase analysis by XRD and Mössbauer spectroscopy are discussed. XRD analysis revealed that the crystallite size (mean coherence length) of iron oxides (mainly γ -Fe₂O₃) in the Fe₂O₃ sample was 30 nm, while in Fe₂O₃/SiO₂ where the ϵ -Fe₂O₃ phase dominated it was only 14 nm. Gd/SiO₂ nanoparticles were found to be completely amorphous, according to XRD. The samples showed various shapes of hysteresis loops and different coercivities. Differences in the saturation magnetization (MS) correspond to the chemical and phase composition of the sample materials. However, we observed that MS was not reached in the case of Fe₂O₃/SiO₂, while for Gd/SiO₂ sample the MS value was extremely low. Therefore we conclude that only unmodified Fe₂O₃ nanoparticles are suitable for intended biosensing application *in vitro* (e.g. detection of viral nucleic acids) and the phase purification of this sample for this purpose is not necessary.

Keywords: Magnetic nanoparticles; iron oxide; gadolinium nanoparticles; silica coating

1. Introduction

Magnetic nanosized particles have already been known for over 50 years, but research into their potential use in medicine and pharmaceuticals is now the hot topic in this domain [1,2]. The unique combination of high magnetization and paramagnetic behaviour opens these materials to a very wide range of applications. Particularly, the possibilities of nanoparticle modification by biologically active compounds to use them in controlled drug delivery systems, as agents in magnetic resonance imaging and for magnetic-induced tumor treatment via hyperthermia are very interesting [3]. Iron oxide based-nanoparticles belong to the most widely used materials in this field, although they have worse magnetic properties, lower saturation magnetization, and lower specific loss of power than Fe and Co nanoparticles which have just started to gain attention for biomedical purposes, too [4]. However, iron oxides have several advantages over Fe and Co nanoparticles, e.g., better oxidative stability, compatibility in nonaqueous systems, and nontoxicity. Among the four well-known crystalline polymorphs of iron(III) oxide (α -Fe₂O₃ as hematite, β -Fe₂O₃, γ -Fe₂O₃ as maghemite and ϵ -Fe₂O₃), maghemite has gained the greatest interest in above mentioned applications [5]. Moreover, magnetite Fe₃O₄ is also very promising candidate as it is biocompatible and biodegradable [6,7].

Several methods are generally employed for iron oxide nanoparticle preparation, including coprecipitation [8], which is preferred due to its simplicity. On the other hand, thermal decomposition [9] seems to give the best control of nanoparticles size and morphology. The resulting physico-chemical properties of nanosized magnetic product obviously depend strongly on the fabrication conditions, especially on material origin, concentration and pH of solution as well as on the mode of thermal treatment used (annealing temperature, atmosphere and rate of heating/cooling). It was found that ferromagnetic low temperature phase γ -Fe₂O₃ can be easily transformed into the antiferromagnetic more stable phase α -Fe₂O₃ when the temperature exceeds 500 °C [10]. Thus it is extremely important to optimize the preparation procedure in order to prevent formation of undesired product(s). The particle size also plays a crucial role. Typical particle sizes for the ferro- to superparamagnetic phase transformation are between 10 and 20 nm for oxides and 1–3 nm for metals [11]. Morales *et al.* observed that the use of polymers in the material synthesis limits the particle size [12]. Ultrasmall magnetic iron oxide nanoparticles (<5 nm) with very uniform size distribution can be also synthesized using the water-in-oil microemulsion method [13].

Recently, more sophisticated Fe₂O₃ nanoparticles were fabricated where the magnetic core was covered by an amorphous silica shell [14]. The frequently used raw materials for Fe₂O₃/SiO₂ preparation are iron salts (chlorides [15], nitrates [16], sulphates [17] etc.) and various silicates (water glass, sodium metasilicate). In the case of the sol-gel preparation technique employing TEOS (tetraethyl orthosilicate) as silica source, it was discovered that the particle size was independent of the silica host matrix porosity, but strongly dependent on the amount of solvent trapped inside the gels [18]. The silica shells could be further modified for better conjugation with various biological molecules such as antibodies, proteins, targeting ligands etc. [19]. From the tumor diseases treatment point of view, –NH₂ and –SH groups are particularly interesting, because they can provide easy

coupling of magnetic nanoparticles with various biologically important molecules such as the promising tumor disease marker called metallothionein [20]. Streptavidin is another important material which can be immobilized on magnetic nanoparticles in order to use them for biosensing purposes [21]. Streptavidin is known for its special affinity towards the vitamin biotin and hence it is suitable for detection of diverse biomolecules in immunoassays, e.g. detection of viral nucleic acids *in vitro*.

Moreover, it was found that the combination of SiO₂ core and protecting coating was useful for designing paramagnetic gadolinium nanoparticles for multimodal contrast agent with optical and magnetic properties [22]. However, the synthesis of such products is often time-consuming, so there is a demand for using rather simpler ways of fabricating magnetic nanoparticles. This paper is aimed at the study of basic magnetic properties of silica coated and non-coated iron oxide prepared with the help of a simple co-precipitation method compared to gadolinium nanoparticles in silica matrix fabricated using a water in oil microemulsion system.

2. Experimental Section

To prepare Fe₂O₃/SiO₂ nanoparticles, we employed an easy co-precipitation method reported previously by Ichianagi *et al.* [23]. Briefly, a 0.05 M aqueous solution of FeCl₂·4H₂O (Fluka) was mixed with 0.02 M aqueous solution of Na₂SiO₃·9H₂O (Reachim) at pH 7. The formed black colored precipitate was washed with distilled water, dried at 80 °C for 15 min and finally air-annealed for 4 hours at 800 °C in an oven.

The following process was applied for the fabrication unmodified Fe₂O₃ magnetic particles: 0.05 M aqueous solution of FeCl₂·4H₂O was mixed with a solution containing 1g/L of K₂CO₃ (Penta) under constant stirring up to pH 7, which resulted in the formation of a black precipitate. After washing and separation, the precipitate was dried at 80 °C for 15 min, then finely crushed in an agate mortar and finally treated thermally at 200 °C in air in an oven for 4 hours.

The process of Gd/SiO₂ nanoparticles synthesis published recently by Santra *et al.* [24] was slightly modified in our work, i.e. without final amine-functionalization and using similar reagents: *N*-[3-(trimethoxysilyl)propyl] ethylenediamine for capturing of paramagnetic Gd³⁺ ions and 3-(trihydroxy-silyl)propyl methylphosphonate monosodium salt solution to produce highly water dispersible nanoparticles. All reagents were purchased from Aldrich, except NH₄OH (Fluka).

Approximate particle size of samples was determined using Scanning Electron Microscopy (SEM, model FEI Quantum 200). For SEM analysis, samples were placed on conductive copper sticking tape. The structure of the samples was checked by X-ray diffraction (XRD) using X'PERT diffractometer from PANalytical and CoK α radiation with qualitative analysis carried out by HighScore software and the JCPDS PDF-2 database. For a quantitative analysis of the XRD patterns, we took HighScore plus with Rietveld structural models based on the ICSD database. ⁵⁷Fe Mössbauer spectra used for phase analysis were measured using ⁵⁷Co/Rh source in standard transmission at room temperature and in a cryostat down to 28 K. Spectrum calibrations were done using α -Fe standard. The computer processing of the spectra yielded intensities *I* of the components (atomic fraction of Fe atoms), their hyperfine inductions *B*_{hf}, isomer shifts δ , quadrupole splittings ΔE_Q , and quadrupole shifts ϵ_Q . The magnetic measurements were carried out using vibrating sample magnetometer at room temperature in an external magnetic field up to 1 T.

3. Results and Discussion

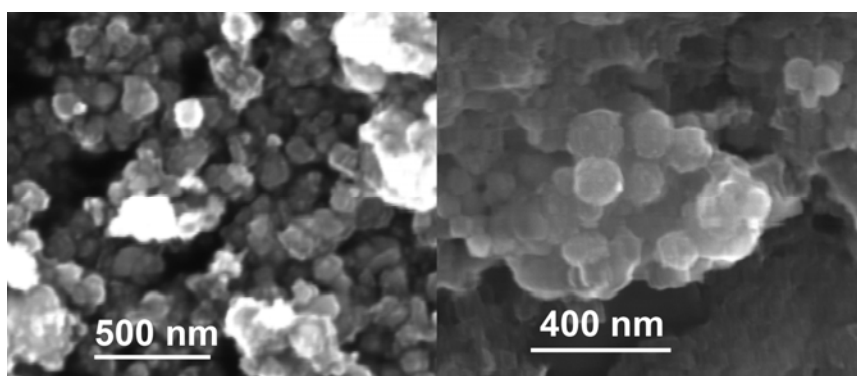
The obtained $\text{Fe}_2\text{O}_3/\text{SiO}_2$ and Fe_2O_3 powders were brownish-black and reddish-brown, respectively, while Gd/SiO_2 nanoparticles were orange due to their doping by fluorescent dye, tris(2,2'-bipyridyl) dichlororuthenium(II) hexahydrate. Only Fe_2O_3 nanoparticles revealed the magnetic properties in water suspension when external magnetic field was applied (Figure 1.).

Figure 1. Magnetic properties illustration of Fe_2O_3 nanoparticles dispersed in water.



SEM analysis demonstrated that the nanoparticles of all prepared samples have particle sizes below 100 nm (Figure 2.). The particles were generally spherical in the shape. However it can be supposed that the size distribution for all samples is rather wide.

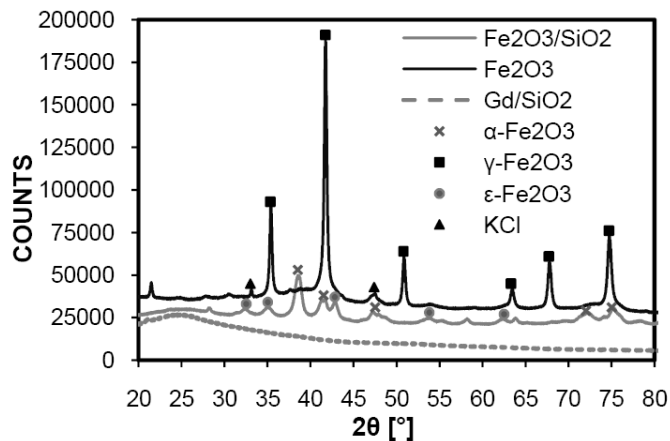
Figure 2. SEM image of Fe_2O_3 (left) and $\text{Gd}^{\text{III}}/\text{SiO}_2$ (right).



According to XRD measurement (XRD patterns of all samples are shown in Figure 3.), $\text{Gd}^{\text{III}}/\text{SiO}_2$ nanoparticles were found to be completely amorphous. The orthorhombic $\epsilon\text{-Fe}_2\text{O}_3$ was observed as majority phase (49 %) together with hematite (24 %) in the case of $\text{Fe}_2\text{O}_3/\text{SiO}_2$ annealed at 800 °C for 4 hours, which is different from the results reported by Ichiyangi *et al.* [25]. The $\epsilon\text{-Fe}_2\text{O}_3$ phase is considered to be an intermediate between maghemite and hematite and it is magnetically very interesting for its high coercive force [26]. The value of mean coherence length corresponding to crystallite size estimated using Rietveld analysis was about 14 nm for both α - and $\epsilon\text{-Fe}_2\text{O}_3$ phases. It can be assumed that there are also very small maghemite or magnetite particles but these were not

detected in XRD spectra probably due to “hiding” of their peaks in the amorphous one belonging to SiO₂ (27 %).

Figure 3. XRD patterns of Fe₂O₃/SiO₂, Fe₂O₃ and Gd^{III}/SiO₂.



The phase analysis carried out from the Mössbauer spectrum (Figure 4) confirmed ϵ -Fe₂O₃ as the dominating iron containing phase (51 %) represented by four sextets with following parameters (see Table 1.). The ϵ -Fe₂O₃ phase was completed by hematite (8 %), superparamagnetic maghemite (19 %, represented by two doublets) and amorphous phase (22 %, represented by a broad sextet).

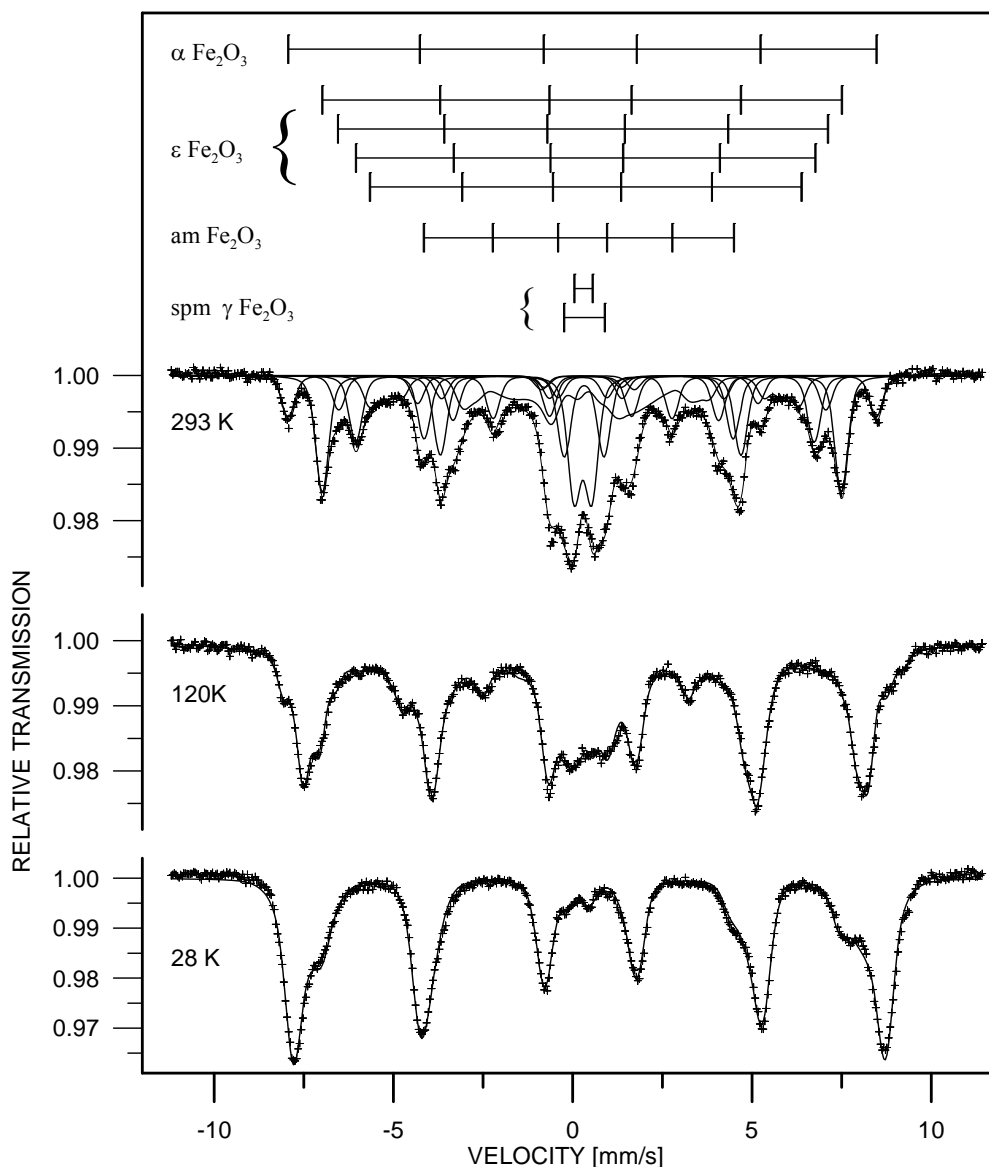
Table 1. Hyperfine parameters deduced from Mössbauer spectrum of Fe₂O₃/SiO₂ measured at 293 K. (c – phase content as atomic fraction of iron atoms, *I* – fraction of the component, *B*_{hf} – hyperfine induction, δ – isomer shift, ϵ_Q – quadrupole splitting, Δw – width of the hyperfine field distribution; spm. – superparamagnetic, am. – amorphous).

Phase	c [%]	Component	<i>I</i>	<i>B</i> _{hf} [T]	δ [mm/s]	ϵ_Q [mm/s]	Δw [T]
ϵ -Fe ₂ O ₃	51±1	1st sextet	0.42±0.01	45.0±0.1	0.37±0.01	−0.25±0.01	-
		2nd sextet	0.12±0.01	42.2±0.2	0.28±0.03	−0.02±0.01	-
		3rd sextet	0.24±0.01	39.7±0.2	0.35±0.01	−0.03±0.01	-
		4th sextet	0.22±0.01	26.8±0.1	0.22±0.01	−0.11±0.01	-
α -Fe ₂ O ₃	8±1	sextet	1.00	51.3±0.1	0.34±0.01	−0.17±0.02	-
γ -Fe ₂ O ₃ spm.	19±1	1st doublet	0.60±0.01	-	0.28±0.01	0.97±0.03	-
		2nd doublet	0.40±0.01	-	0.32±0.01	2.21±0.04	-
am.	22±1	sextet	1.00	11.9±0.3	0.35±0.04	−0.20±0.06	7.3±0.8

The superparamagnetic behaviour of the maghemite is documented by the measurement of the Mössbauer spectra at various temperatures (shown in Figure 4.). The doublets ascribed to the maghemite splitted continuously to sextets when the sample temperature decreased below the blocking temperature. The broad interval of the blocking temperature indicates broad size distribution of the maghemite nanoparticles. The amorphous phase represents probably surfaces, interfacial regions, fine particles slightly below blocking temperature and particles with perturbed oxygen stoichiometry of the

magnetic phases mentioned above. Generally, all values of relative intensities and hyperfine parameters agree with the data reported in literature, e.g. [10,27,28].

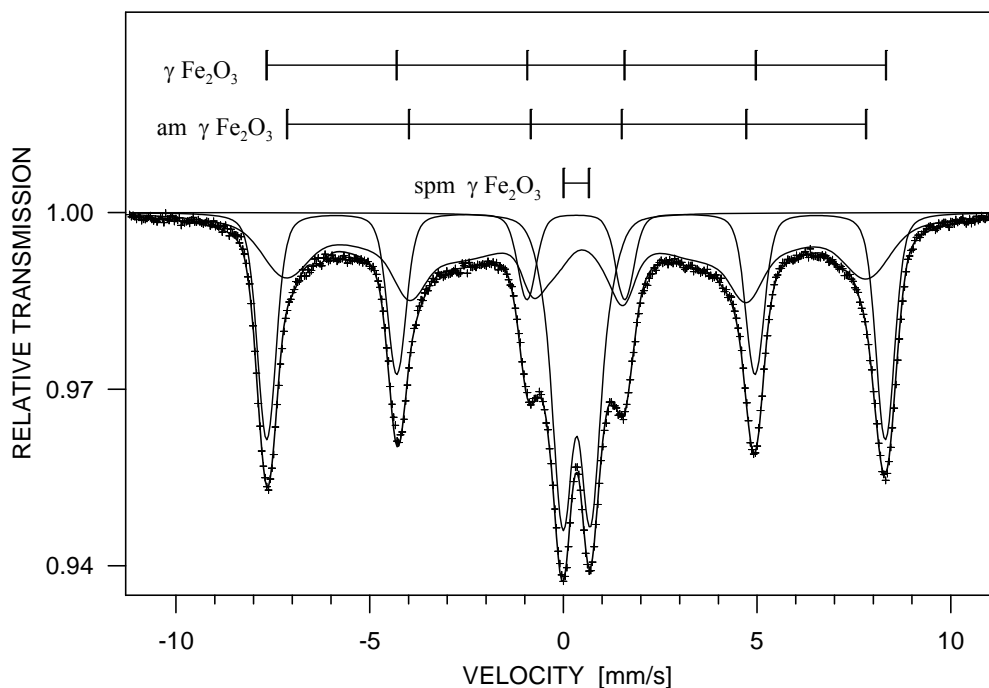
Figure 4. Mössbauer spectrum of $\text{Fe}_2\text{O}_3/\text{SiO}_2$ sample depending on measurement temperature changes.



The prepared unmodified Fe_2O_3 powder consisted of 60 % iron oxide, 30 % of sylvite (KCl) and small portion of amorphous phase. The mean coherence length of iron oxide phase was about 30 nm. Since X-ray powder diffraction cannot distinguish between maghemite and magnetite nanoparticles, Mössbauer spectroscopy analysis was performed to distinguish these crystallographic modifications (Figure 5). The results showed the maghemite phase being dominant (36 %), as represented with a sextet of $B_{\text{hf}} = 49.6 \pm 0.1$ T, $\delta = 0.32 \pm 0.01$ mm/s, $\epsilon_Q = 0.01 \pm 0.01$ mm/s. Besides that a small amount of magnetite Fe_3O_4 (6 %, two sextets $B_{\text{hf}} = 48.1 \pm 0.1$ T, $\delta = 0.32 \pm 0.02$ mm/s, $\epsilon_Q = 0.06 \pm 0.03$ mm/s and $B_{\text{hf}} = 45.1 \pm 0.1$ T, $\delta = 0.67 \pm 0.02$ mm/s, $\epsilon_Q = -0.07 \pm 0.03$ mm/s) and some amorphous phase which is probably of the same origin as in the case of $\text{Fe}_2\text{O}_3/\text{SiO}_2$ were detected. Generally it is very difficult to distinguish between a true amorphous Fe_2O_3 phase and nanocrystalline polymorphs exhibiting very

small particle size [29]. Thus for their more precise identification, a measurement in external magnetic field should be done. Moreover, a superparamagnetic or paramagnetic component was detected in this sample.

Figure 5. Mössbauer spectrum of Fe_2O_3 sample.



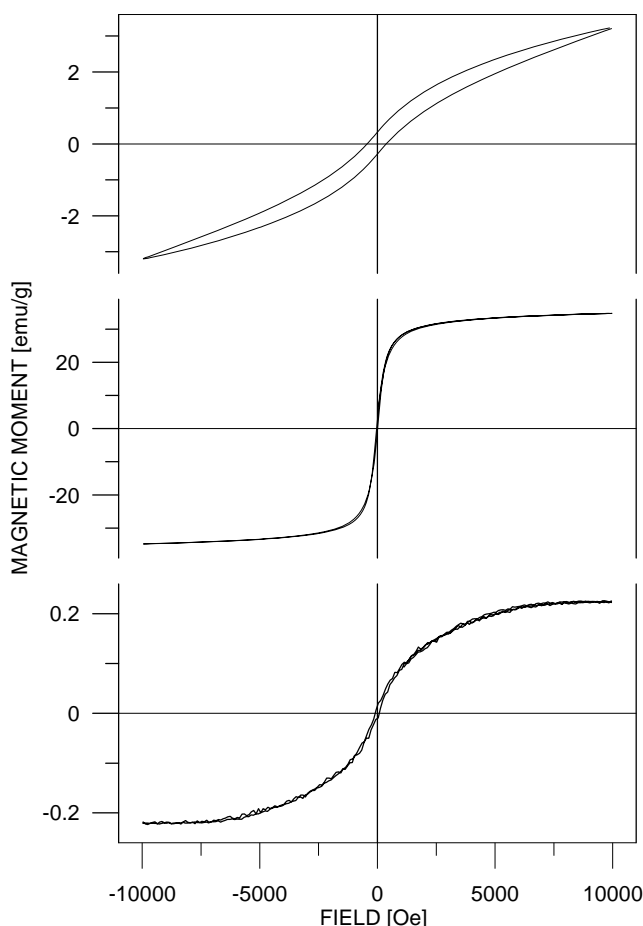
Magnetic hysteresis loops taken at room temperature are shown in Figure 6. The hysteresis loop (HL) of $\text{Fe}_2\text{O}_3/\text{SiO}_2$ nanoparticles documents that we were not able to saturate the sample in the field of 10 kOe. Therefore we can only report the parameters of the minor HL at the field of 10 kOe: moment of 3 emu/g and corresponding coercive field of 400 ± 20 Oe. It indicates that the phase did not reach the particle size where its shape and magnetocrystalline anisotropies cause high coercivity. The moment value could be recalculated to the pure $\epsilon\text{-Fe}_2\text{O}_3$ from the phase composition given by XRD and Mössbauer phase analysis. In order to reach saturation on the HL, a strong external field is necessary [30]. On the other hand, such a strong external field would influence the mutual interactions of the $\epsilon\text{-Fe}_2\text{O}_3$ and the (super)paramagnetic phase (at room temperature) which is present in the sample according to the Mössbauer spectrum measurement.

The HL shape of the Fe_2O_3 nanoparticles corresponds well to an assembly of individual magnetic particles with mutual dipolar interaction. The value of magnetic moment at 10 kOe is about 35 emu/g. Taking into account the results of phase analysis, i. e. the contents of sylvite ($\sim 30\%$ according to XRD) and (super)paramagnetic phase ($\sim 25\%$ from Mössbauer spectrum), we can roughly estimate the moment of $\gamma\text{-Fe}_2\text{O}_3$ nanoparticles to be 66 emu/g. This is a comparable value to that reported in [31] and to the one inside the range of values 60–80 emu/g published in [32]. The coercive field derived from the HL is about 30 ± 5 Oe and it roughly agrees with data described in [33].

The HL parameters of $\text{Gd}^{\text{III}}/\text{SiO}_2$ sample are the moment of 0.23 emu/g at 10 kOe and coercive field of 70 ± 5 Oe. Estimation of the magnetic moment to a pure Gd phase from the expected phase composition given by chemical composition would increase the moment value approximately two

times. This is still substantially lower value than the one reported for bulk Gd (139 emu/g) [34]. It should be mentioned that Curie temperature for pure Gd is about 289 K. A comparison to non-protected Gd nanoparticles or thin films (e.g. to those described in [35]) would not be correct because of probably important differences in Gd sample oxidations during the most frequently applied preparation techniques and/or handling of the samples in ambient atmosphere.

Figure 6. Magnetization curves of Fe₂O₃/SiO₂ (top), Fe₂O₃ (center) and Gd^{III}/SiO₂ (bottom).



4. Conclusions

In this article we report the synthesis of iron oxides and gadolinium nanoparticles using coprecipitation and water in oil microemulsion methods, respectively. The XRD phase analysis showed interesting differences in development of crystallinity and mean coherent lengths. While in Fe bearing materials crystalline phase peaks were detected, the Gd based sample only showed an amorphous diffraction. The ϵ -Fe₂O₃ was found to be the dominating crystalline phase in the Fe₂O₃/SiO₂ sample. This result was confirmed by Mössbauer phase analysis. Maghemite dominated in the unmodified Fe₂O₃ powder sample. The magnetization curves corresponded to assemblies of individual magnetic particles with mutual dipolar interaction separated by another nonmagnetic phase, e.g. SiO₂ and KCl. The samples exhibited clear differences in saturation magnetization which can be ascribed mainly to the different chemical composition and magnetic moments of Fe and Gd and their phases. Since ϵ -Fe₂O₃ phase did not reach a particle size where its shape and magnetocrystalline anisotropies cause

high coercivity, one of the objectives in future work will be to increase the coercive force, as well as the amount of this phase by prolongation of sample annealing time.

We found that only the Fe₂O₃ sample is suitable for practical medical applications due to its sufficiently high value of saturation magnetization and attraction to magnet ability. Despite the fact that this material does not consist of one phase, it can be used for biosensing purposes *in vitro*, for example for detection of viral nucleic acids (influenza, jaundice) with the help of streptavidin-conjugated magnetic nanoparticles. We expect the surface of this sample can be modified further by specific sequences of nucleic acids complementary to viral DNA in order to detect the serious diseases such as cancer, HIV, bird flu etc. We also propose these nanoparticles can be coated by chicken antibodies against metallothionein, which can specifically interact with the target molecule.

Acknowledgements

The financial support from the grant KAN 208130801 is highly acknowledged. Many thanks also to FEI Company for providing of SEM analysis.

References and Notes

1. Arruebo, M.; Fernandez-Pacheco, R.; Ibarra, M.R.; Santamaria, J. Magnetic nanoparticles for drug delivery. *Nano Today* **2007**, *2*, 22–32.
2. Lu, A.H.; Salabas, E.L.; Schuth, F. Magnetic nanoparticles: Synthesis, protection, functionalization, and application. *Angew. Chem.-Int. Edit.* **2007**, *46*, 1222–1244.
3. Kumar, C.S.S.R. *Biofunctionalization of Nanomaterials*; Wiley-VCH: Weinheim, 2005; Vol. 1, pp. 72–98.
4. Hutten, A.; Sudfeld, D.; Ennen, I.; Reiss, G.; Hachmann, W.; Heinzmann, U.; Wojczykowski, K.; Jutzi, P.; Saikaly, W.; Thomas, G. New magnetic nanoparticles for biotechnology. *J. Biotechnol.* **2004**, *112*, 47–63.
5. Tucek, J.; Zboril, R.; Petridis, D. Maghemite nanoparticles by view of Mossbauer spectroscopy. *J. Nanosci. Nanotechnol.* **2006**, *6*, 926–947.
6. Gupta, A.K.; Gupta, M. Synthesis and surface engineering of iron oxide nanoparticles for biomedical applications. *Biomaterials* **2005**, *26*, 3995–4021.
7. Xie, J.; Xu, C.J.; Xu, Z.C.; Hou, Y.L.; Young, K.L.; Wang, S.X.; Pourmond, N.; Sun, S.H. Linking hydrophilic macromolecules to monodisperse magnetite (Fe₃O₄) nanoparticles via trichloro-s-triazine. *Chem. Mat.* **2006**, *18*, 5401–5403.
8. Tang, D.P.; Yuan, R.; Chai, Y.Q. Direct electrochemical immunoassay based on immobilization of protein-magnetic nanoparticle composites on to magnetic electrode surfaces by sterically enhanced magnetic field force. *Biotechnol. Lett.* **2006**, *28*, 559–565.
9. Zboril, R.; Mashlan, M.; Petridis, D. Iron(III) oxides from thermal processes-synthesis, structural and magnetic properties, Mossbauer spectroscopy characterization, and applications. *Chem. Mat.* **2002**, *14*, 969–982.

10. Ortega, D.; Garitaonandia, J.S.; Barrera-Solano, C.; Ramirez-Del-Solar, M.; Blanco, E.; Dominguez, M. gamma-Fe₂O₃/SiO₂ nanocomposites for magneto-optical applications: Nanostructural and magnetic properties. *J. Non-Cryst. Solids* **2006**, *352*, 2801–2810.
11. Batlle, X.; Labarta, A. Finite-size effects in fine particles: magnetic and transport properties. *J. Phys. D-Appl. Phys.* **2002**, *35*, R15–R42.
12. Morales, M.A.; Finotelli, P.V.; Coaquira, J.A.H.; Rocha-Leao, M.H.M.; Diaz-Aguila, C.; Baggio-Saitovitch, E.M.; Rossi, A.M. *In situ* synthesis and magnetic studies of iron oxide nanoparticles in calcium-alginate matrix for biomedical applications. *Mater. Sci. Eng. C-Biomimetic Supramol. Syst.* **2008**, *28*, 253–257.
13. Santra, S.; Tapeç, R.; Theodoropoulou, N.; Dobson, J.; Hebard, A.; Tan, W.H. Synthesis and characterization of silica-coated iron oxide nanoparticles in microemulsion: The effect of nonionic surfactants. *Langmuir* **2001**, *17*, 2900–2906.
14. De Palma, R.; Trekker, J.; Peeters, S.; Van Bael, M.J.; Bonroy, K.; Wirix-Speetjens, R.; Reekmans, G.; Laureyn, W.; Borghe, G.; Maes, G. Surface modification of gamma-Fe₂O₃@ SiO₂ magnetic nanoparticles for the controlled interaction with biomolecules. *J. Nanosci. Nanotechnol.* **2007**, *7*, 4626–4641.
15. Iida, H.; Takayanagi, K.; Nakanishi, T.; Kume, A.; Muramatsu, K.; Kiyohara, Y.; Akiyama, Y.; Osaka, T. Preparation of Human Immune Effector T Cells Containing Iron-Oxide Nanoparticles. *Biotechnol. Bioeng.* **2008**, *101*, 1123–1128.
16. Khalil, K.M.S.; Mahmoud, H.A.; Ali, T.T. Direct formation of thermally stabilized amorphous mesoporous Fe₂O₃/SiO₂ nanocomposites by hydrolysis of aqueous iron (III) nitrate in sols of spherical silica particles. *Langmuir* **2008**, *24*, 1037–1043.
17. Srinivasan, B.; Huang, X.F. Functionalization of magnetic nanoparticles with organic molecules: Loading level determination and evaluation of linker length effect on immobilization. *Chirality* **2008**, *20*, 265–277.
18. Cannas, C.; Concas, G.; Gatteschi, D.; Musinu, A.; Piccaluga, G.; Sangregorio, C. How to tailor maghemite particle size in gamma-Fe₂O₃-SiO₂ nanocomposites. *J. Mater. Chem.* **2002**, *12*, 3141–3146.
19. Ichiyanagi, Y.; Moritake, S.; Taira, S.; Setou, M. Functional magnetic nanoparticles for medical application. *J. Magn. Magn. Mater.* **2007**, *310*, 2877–2879.
20. Fabrik, I.; Krizkova, S.; Huska, D.; Adam, V.; Hubalek, J.; Trnkova, L.; Eckschlager, T.; Kukacka, J.; Prusa, R.; Kizek, R. Employment of electrochemical techniques for metallothionein determination in tumor cell lines and patients with a tumor disease. *Electroanalysis* **2008**, *20*, 1521–1532.
21. Liu, H.L.; Sonn, C.H.; Wu, J.H.; Lee, K.M.; Kim, Y.K. Synthesis of streptavidin-FITC-conjugated core-shell Fe₃O₄-Au nanocrystals and their application for the purification of CD4(+) lymphocytes. *Biomaterials* **2008**, *29*, 4003–4011.
22. Gerion, D.; Herberg, J.; Bok, R.; Gjersing, E.; Ramon, E.; Maxwell, R.; Kurhanewicz, J.; Budinger, T.F.; Gray, J.W.; Shuman, M.A.; Chen, F.F. Paramagnetic silica-coated nanocrystals as an advanced MRI contrast agent. *J. Phys. Chem. C* **2007**, *111*, 12542–12551.
23. Ichiyanagi, Y.; Kimishima, Y. Structural, magnetic and thermal characterizations of Fe₂O₃ nanoparticle systems. *J. Therm. Anal.* **2002**, *69*, 919–923.

24. Santra, S.; Bagwe, R.P.; Dutta, D.; Stanley, J.T.; Walter, G.A.; Tan, W.; Moudgil, B.M.; Mericle, R.A. Synthesis and characterization of fluorescent radio-opaque and paramagnetic silica nanoparticles for multimodal bioimaging applications. *Adv. Mater.* **2005**, *17*, 2165–2169
25. Ichiyanagi, Y.; Uozumi, T.; Kimishima, Y. Magnetic properties of Fe₂O₃ nanoparticles. *Trans. Mat. Res. Soc. Jpn.* **2001**, *26*, 1097–1100.
26. Ding, Y.; Morber, J.R.; Snyder, R.L.; Wang, Z.L. Nanowire structural evolution from Fe₃O₄ to epsilon-Fe₂O₃. *Adv. Funct. Mater.* **2007**, *17*, 1172–1178.
27. Long, G.J.; Grandjean, F. *Mössbauer Spectroscopy Applied to Magnetism and Materials Science*. Plenum Press: New York, 1993; Vol. 1, pp. 115–159.
28. Tronc, E.; Chaneac, C.; Jolivet, J.P. Structural and magnetic characterization of epsilon-Fe₂O₃. *J. Solid State Chem.* **1998**, *139*, 93–104.
29. Machala, L.; Zboril, R.; Gedanken, A. Amorphous iron(III) oxide - A review. *J. Phys. Chem. B* **2007**, *111*, 4003–4018.
30. Popovici, M.; Gich, M.; Niznansky, D.; Roig, A.; Savii, C.; Casas, L.; Molins, E.; Zaveta, K.; Enache, C.; Sort, J.; de Brion, S.; Chouteau, G.; Nogues, J. Optimized synthesis of the elusive epsilon-Fe₂O₃ phase via sol-gel chemistry. *Chem. Mat.* **2004**, *16*, 5542–5548.
31. Tartaj, P.; Serna, C.J. Microemulsion-assisted synthesis of tunable superparamagnetic composites. *Chem. Mat.* **2002**, *14*, 4396–4402.
32. Cornell, R.M.; Schwertmann, U. *The Iron Oxides: Structure, Properties, Reactions, Occurrence and Uses*; VCH: New York, 1996; p. 117.
33. Wohlfarth, E.P. *Ferromagnetic Materials*; North-Holland: Amsterdam, 1980; Vol. 2, p. 442.
34. Wohlfarth, E.P. *Ferromagnetic Materials*; North-Holland: Amsterdam, 1980; Vol. 2, p. 512.
35. O'Shea, M.J.; Perera, P. Influence of nanostructure (layers and particles) on the magnetism of rare-earth materials. *J. Appl. Phys.* **1999**, *85*, 4322–4324.

© 2009 by the authors; licensee Molecular Diversity Preservation International, Basel, Switzerland. This article is an open-access article distributed under the terms and conditions of the Creative Commons Attribution license (<http://creativecommons.org/licenses/by/3.0/>).